THEORETICAL ELASTIC STIFFNESS TENSOR AT HIGH CRACK DENSITY

YANRONG HU and GEORGE A. MCMECHAN

Center for Lithospheric Studies, The University of Texas at Dallas, 800 W. Campbell Road, Richardson, TX 75080-3021, U.S.A.

(Received July 20, 2009; revised version accepted September 14, 2009)

ABSTRACT

Hu, Y. and McMechan, G.A., 2010. Theoretical elastic tensor models at high crack density. *Journal of Seismic Exploration*, 19: 43-68.

Elastic stiffness tensor values in cracked rocks depend on the crack density, and on the shapes, fluid content, orientation, and spatial distribution of the cracks. The mathematical expression of anisotropy is embedded in the elastic stiffness tensor. Thus, in reservoir characterization by anisotropic seismic modeling, inversion and interpretation, a key step is to represent the rock properties in terms of the equivalent anisotropic elastic stiffness tensor.

We compare the strengths, limitations, and relationships between the anisotropic elastic stiffness tensor elements predicted for a transversely isotropic medium with a horizontal symmetry axis,using a variety of theoretical formulations, including equivalent single inclusion approximations, smoothing, self consistent approximation (SCA), differential effective medium (DEM) methods, linear slip (LS), and T-matrix methods. These formulations differ in their crack parametrizations, the assumptions and approximations involved, and the corresponding consequences of these.

All the formulations involve theoretical extrapolations. Absolute accuracy is not known for high crack density because, while there is substantial internal consistency between the theoretical results when crack interactions are included, there is to date, only limited external validation in terms of physical and numerical experiments at high crack densities.At high crack densities, where crack interactions are important, physically reasonable values are expected to be predicted only by the formulations that implicitly or explicitly consider these effects. These methods are the SCA, DEM, LS and T-matrix methods. For a coal example, all these four methods predict similar elastic stiffness tensor values up to volume crack densities of ≤ 0.3, beyond which, the spatial distribution of cracks in the various models becomes increasingly important. In a medium with perfectly aligned fractures, the shear modulus normal to the symmetry plane shows the greatest relative variation between models at high crack density.

KEYWORDS: elastic tensor, anisotropy, crack density.

0963-0651/10/$5.00

INTRODUCTION

The presence of fractures in rocks affects the propagation of seismic waves in a variety of ways. If the fractures are aligned, the velocities of seismic waves will be functions of polarization directions, resulting in anisotropy. Fractures generate seismic anisotropy, unless the fracture orientations are random. The simplest type of seismic anisotropy, transverse isotropy (TI), can be caused by aligned fractures in an isotropic host rock. A TI medium has five independent elements in the elastic stiffness tensor (Thomsen, 1986). The anisotropic elastic stiffness tensor is the mathematical expression of anisotropy. Thus, a key step is to represent the crack properties in terms of the equivalent anisotropic elastic stiffness tensor. The main motivation for the present work is to produce the input needed for numerical simulation of the seismic responses of anisotropic media (e.g., Ramos-Martínez and McMechan, 2000). Thus we limit our examples to a single set of aligned cracks, rather than considering an assemblage of randomly oriented cracks that is isotropic on the macro scale.

Seismic wavelengths are typically substantially (tens of times) larger than the fracture dimensions (Liu et al., 2000). Dimensions of fractures that are likely to cause seismic anisotropy usually range from microns to a few meters. A fracture may be composed of a single large crack or several small cracks (Liu et al., 2000). This implies that the effective elastic anisotropy is insensitive to the size of the individual cracks (Crampin, 1994). A fractured medium can be modeled as an effective elastic medium with anisotropic symmetry corresponding to the particular crack distribution and orientations. Much of the theoretical basis for the study of moduli of cracked media has been done in the solid mechanics and mechanical engineering communities (e.g., Bristow, 1960; Kachanov, 1980, 1992, 1994). Early geophysical examples are in Walsh (1965a, b).

Because of the importance of the effective anisotropic elastic properties for seismic modeling, inversion and interpretation, several theoretical models have been proposed. These models include the equivalent single inclusion (Eshelby, 1957), self consistent approximation (SCA) (O'Connell and Budiansky, 1974; Budiansky and O'Connell, 1976; Willis, 1977), differential effective medium (DEM) methods (Nishizawa, 1982; Sheng, 1990; Hornby et al., 1994), Hudson's smoothing methods (Hudson, 1980, 1981, 1994), linear slip (LS) methods (Schoenberg, 1980; Schoenberg and Douma, 1988; Schoenberg and Sayers, 1995; Sayers and Kachanov, 1995; Hudson and Liu, 1999; Liu et al., 2000) and T-matrix methods (Jakobsen et al., 2003; Jakobsen, 2004). Although these formulations each have their own assumptions, parametrizations, advantages, and limitations, some of them evolved from others and hence have inherited characteristics.

Crack density (Kachanov, 1980) is common to all these theories and is critical, both to the potential hydrocarbon storage and productivity of the reservoir rocks, and to the resulting seismic anisotropy. The dimensionless volume crack density $\varepsilon = \nu\langle a^3 \rangle$, where ν is the number crack density (the number of cracks per unit volume of rock), a is the crack radius, and $\langle\rangle$ denotes an average (O'Connell and Budiansky, 1974; Hudson, 1980). Most studies of seismic anisotropy are limited to weak anisotropy [which means that Thomsen's (1986) anisotropy parameters are much less than 1.0, or $\varepsilon < 0.1$ for aligned cracks].

Strong seismic anisotropy may be present in a variety of rocks if the density of the aligned cracks is high. Many field investigations and lab experiments reveal that large crack density is common (Table 1). The crack density is independent of the aperture (thickness) of the cracks. Cracks with very small aperture can occur in dense swarms with high crack density without the rock being broken or losing cohesion. The confining stress keeps severely fractured rock, with high crack density, integrated, while overpressure fluid keeps cracks open (Sayers, 1994). Therefore, fractured rock will not necessarily be fragmented or lose coherence if $\varepsilon > 0.1$, which is the limit suggested by Crampin (1984) for a Poisson solid.

Table 1. Thomsen's parameters (ϵ, γ), and crack density for some rocks. The ϵ here should not be confused with the ε used for crack density elsewhere in this paper.

Lithology	References	ϵ	γ
Limestone	Crampin et al. (1980)	0.27	-
	Gupta (1973)	0.65	0.34
	Jakobsen and Johansen (2000)	0.16	0.24
	Wang (2002)	0.20	0.12
Granite	Nur and Simmons (1969)	0.30	0.20
	Hadley (1975)	0.20	0.28
	Lo et al. (1986)	0.30	0.03
	David et al. (1999)	crack density = 0.30	
Coal	Shuck et al. (1996)	crack density = 0.30	
Marble	Peacock et al. (1994)	crack density = 0.42	

An inclusion may have any shape but, following Eshelby's (1957) model, we restrict it to an ellipsoid. A crack is usually a flat inclusion with low aspect ratio, which is the ratio of thickness to length of the ellipsoid. In Eshelby's model, the cracks (inclusions) are sufficiently separated from each other that the crack-crack interaction can be neglected. This method gives only first-order predictions; the effective elastic stiffness tensor elements are linearly dependent on the crack density.

In Hudson's (1980, 1981) second-order approximation (smoothing) methods, the effective elastic stiffness tensor elements are functions containing terms up to the second power of crack density. Although it is widely used, this method is still limited to small crack densities and small crack aspect ratios (penny-shaped cracks); crack interactions are estimated when they are not very strong.

The SCA and DEM methods (Vavakin and Salganik, 1975; Hashin, 1988) can be applied to high crack density because crack-crack interactions are taken into account. Although SCA and DEM are not physically-based models (Hudson, 1981; Douma, 1988; Cheng, 1993), they allow representation of the elastic stiffness tensor components as a function of crack density. Another alternative is presented by Benveniste (1986), who generalizes Mori and Tanaka's (1973) average elastic energy approach to extend Eshelby's equivalent inclusion formulation to consider interaction between inclusions.

Linear slip methods (Schoenberg, 1980; Liu et al., 2000) are for fracture zones composed of small, aligned, interacting circular cracks or circular asperities and are supposed to be suitable for high crack density. The effect of an asperity is large, even if it is small in size (Sevostianov and Kachanov, 2001).

The T-matrix methods (Jakobsen et al., 2003) use the T-matrix to represent Eshelby's (1957) single inclusion model. Similar representations are used in the first-order formulations. Two-point correlation functions approximate nearest neighbor crack interactions. Hence the T-matrix methods are also suitable for high crack density. On the other hand, the T-matrix model is developed for a specific spatial pattern of cracks; the applicability to other patterns remains unclear.

Physical experiments performed under controlled conditions may be used to evaluate theoretical models of anisotropic elastic properties. Unfortunately, most published physical experiments (e.g., Rathore et al., 1991; Ass'ad et al., 1992; Ass'ad et al., 1993a, b; Peacock et al., 1994) have tested only Hudson's smoothing method; Rathore et al. (1994) also compare with Thomsen's (1995) model. If the host rock is a Poisson's solid containing dry cracks with aspect

ratio of ~ 0.05, the crack density limit of validity of Hudson's method, suggested by these researchers is ~ 0.1.

Another alternative to evaluating theoretical models is numerical simulation of moduli for specific realizations of cracked media. Examples include Grechka and Kachanov (2006a, b, c), Kachanov (1992), Mauge and Kachanov (1994), Saenger and Shapiro (2002), and Saenger et al. (2004). This numerical approach is the most general and the most accurate that is available, but is also the most expensive and still has various contentious issues (Grechka, 2007; Saenger et al., 2006; Saenger, 2007), so there is still substantial value in comparative evaluations of the existing theoretical solutions.

When waves of seismic frequency propagate in (partially or fully) fluid-saturated, fractured rock, attenuation may be caused by inter- or intra-fracture fluid flow, driven by displacements produced by seismic waves. Under these conditions, the rock is viscoelastic, which is beyond the scope of this study. The purpose of this paper is to compare and evaluate the elastic stiffness tensor components, predicted by existing methods for crack densities $\varepsilon > 0.1$, and to understand their strengths, limitations, and relationships. The resulting effective elastic stiffness tensors may be used as the input to numerical simulations of the seismic responses of anisotropic models associated with specific crack characteristics; the latter is also beyond the scope of the present paper, and is presented by Hu (2008).

SUMMARY OF THEORIES

The main theoretical methods for predicting effective elastic stiffness tensors for fractured rocks are equivalent inclusion methods, self consistent methods, differential effective medium methods, smoothing methods, linear slip methods, and T-matrix methods. The salient characteristics of each are considered in turn, in the following subsections. Mori and Tanaka's (1973) approach could also be considered, but we omit it as it is less commonly used in geophysics; this model is non-linear in the number crack density, but ignores crack interactions. We also do not explicitly consider the related,non-interaction approximation (NIA) of Kachanov (1992) as that is a variant of the first-order linear slip formulation.

Eshelby's equivalent inclusion method

Eshelby (1957) proposes an exact solution for a single inclusion (Fig. 1) that is used to approximate an equivalent model of multiple, non-interacting inclusions. The inclusion is modeled as an ellipsoidal crack with principal axes 2a, 2b, and 2c. The shape of the inclusion can be expressed as $x_1^2/a^2 + x_2^2/b^2 +$

$x_3^2/c^2 = 1$. If a = b, then the inclusion has spheroidal shape with circular cross section of diameter 2b and thickness 2a (Fig. 1). α_1 = c/a is the crack aspect ratio. If $\alpha_1 = 1$, the inclusion is spherical; if $\alpha_1 > 1$, the inclusion is prolate; if $\alpha_1 < 1$, the inclusion is oblate. The ellipsoidal inclusion is representative of stress-induced cracks, deformed pores or vugs, or flat mineral grains (e.g. mica or clay minerals, which can be considered as inclusions filled with minerals). Inclusion is a more general term so a crack can be considered as an inclusion with small aspect ratio.

Eshelby's (1957) method ignores all inclusion-inclusion interactions. It is a non-interacting approximation as the dilute inclusions are sufficiently separated that interactions between them can be ignored. The change of the elastic field caused by the existence of one inclusion does not affect the elastic energy of the other inclusions (Eshelby, 1957). It also ignores the influence of the inclusions on the elastic energy of the matrix, because the volume change of the matrix caused by the presence of an inclusion is very small.

Under the condition of keeping constant displacement and constant strain on the surface of the inclusions, the total energy, of a sample that consists of an isotropic solid matrix with an ellipsoidal inclusion that is small compared to a typical seismic wavelength, is the sum of the elastic energy contributed by the matrix, and the change in the energy contributed by the crack. Eshelby (1957) gives incomplete expressions and Cheng (1978) completes them, in the form

$$\mathbf{C}^* = \mathbf{C}^0 - \phi\mathbf{C}^1 \quad , \tag{1}$$

where $\mathbf{C}^*$ is the effective elastic stiffness tensor of the rock matrix containing the inclusion, ϕ is the inclusion porosity, and $\mathbf{C}^0$ is the elastic stiffness tensor of the host rock. $\mathbf{C}^1$ is the contribution of the individual inclusions, and is a function of the elastic stiffness tensor of the matrix, the shape (the aspect ratio), and the orientation of the ellipsoidal inclusions, and the elastic stiffness tensor of the infill of the inclusions (Cheng, 1978, 1993). Eq. (1) indicates that the effective elastic stiffness tensor is linearly dependent on the inclusion porosity ϕ if all inclusions are uniform, having same shape, orientation and infill. The stiffness also depends linearly on the volume inclusion density ε [as $\phi = (4\pi/3)\varepsilon\alpha_1$]. The dependence of $\mathbf{C}^*$ on α_1 is not linear as α_1 also appears in $\mathbf{C}^1$.

Self consistent approximation (SCA) methods

The SCA methods are proposed by O'Connell and Budiansky (1974, 1977) and Budiansky and O'Connell (1976) for randomly oriented cracks (which is an isotropic medium), and are modified by Hoening (1979) for cracks aligned parallel to the isotropy plane. A single inclusion of the self consistent model is same as in Eshelby's model, but the crack concentration is non-dilute. The SCA

model always accounts for crack-crack interactions, and Eshelby's model never does. The SCA model is iterative, with cracks gradually added to a previous effective medium containing previously added cracks.

Willis (1977) and Hornby et al. (1994) propose the SCA expression:

$$\mathbf{C}_*^{SC} = \sum_{n=1}^{N} \phi_n \mathbf{C}^n [\mathbf{I}_2 + \mathbf{G}(\mathbf{C}^n - \mathbf{C}^{SC})]^{-1} \{ \sum_{p=1}^{N} \phi_p [\mathbf{I}_2 + \mathbf{G}(\mathbf{C}^p - \mathbf{C}^{SC})]^{-1} \}^{-1} \quad , \qquad (2)$$

where $\mathbf{C}_*^{SC}$ and $\mathbf{C}^{SC}$ are the effective elastic stiffness tensors, after and before, an iteration, respectively. The composite materials are composed of N components (including the matrix), with different shapes and materials of inclusions, $\mathbf{C}^n$ (or $\mathbf{C}^p$) is the elastic stiffness Voigt tensor of the n-th (or p-th) component, ϕ_n (or ϕ_p) is the inclusion porosity of the n-th (or p-th) component, $\mathbf{G}$ is a fourth-rank tensor [given by Lin and Mura (1973)] that is related to Eshelby's tensor $\mathbf{S}$ by $\mathbf{S} = \mathbf{G}\mathbf{C}_*$, and $\mathbf{I}_2$ is a second-rank identity tensor. Thus, eq. (2) says that the effective elastic stiffness tensor of the composite is a combination of the elastic stiffness tensors of the elements, each weighted by its inclusion porosity ϕ.

The host rock is not necessarily isotropic (Eshelby, 1957). Lin and Mura (1973) give expressions to calculate the tensor $\mathbf{G}$ in eq. (2) for a transversely isotropic matrix. This tensor may be associated with vertically aligned flat inclusions, minerals, or clay particles, which indicates that the SCA method has wide applications. The elastic stiffness tensor of this effective medium is that of the anisotropic matrix that is produced by the inclusions already added. This matrix is used as the input, to which another dilute increment of inclusions is added. Then the new elastic stiffness tensor is calculated. This scheme is called self consistent and is an iterative solution for a non-dilute inclusion concentration, obtained by accumulation of inclusions. There is no explicit assumption made in SCA about the statistical distribution of cracks. However, the inclusions are implicitly required to be randomly located and statistically evenly distributed.

Differential effective medium (DEM) method

Salganik (1973), Nishizawa (1982), Hashin (1988), Sheng (1990) and Hornby et al. (1994) propose differential effective medium methods (DEM). DEM is similar to SCA, except that, at each iteration, the change of effective elastic stiffness tensor (rather than a new effective elastic stiffness tensor) is calculated. In this way, crack-crack interactions are included approximately in the DEM (Hudson, 1980; Cheng, 1993). Thus, the elastic properties for models

with non-dilute inclusions can be obtained, provided that the cumulative errors resulting from the iterative calculations do not influence the results. For the inclusion model described above for the SCA method, Hornby et al. (1994) propose an expression to calculate the change of effective elastic stiffness tensor ($\Delta\mathbf{C}^i$):

$$\Delta[\mathbf{C}^{DEM}(\phi)] = [\Delta\phi^i/(1 - \phi)][\mathbf{C}^i - \mathbf{C}^{DEM}(\phi)]\{\mathbf{I} + \mathbf{G}[\mathbf{C}^i - \mathbf{C}^{DEM}(\phi)]\}^{-1} , \quad (3)$$

where $\mathbf{C}^{DEM}(\phi)$ is the effective elastic stiffness tensor obtained from the previous iteration, $\Delta[\mathbf{C}^{DEM}(\phi)]$ is the increment of the elastic stiffness tensor, $\Delta\phi^i$ is the new inclusion concentration (of type i) added to the matrix with the previously added inclusion concentration ϕ, and $\mathbf{G}$ is Lin's tensor [see eq. (2)].

DEM gives a model similar to SCA, but uses a different effective scheme to estimate the crack-crack interaction. Because the specific distribution of cracks is not included, DEM is also non-deterministic. Both the SCA and DEM methods are implemented for orientation distributions other than random or strictly aligned.

Hudson's first- and second-order (smoothing) methods

Hudson (1980, 1981, 1986) proposes smoothing methods, by averaging equations of motion over the cracks, to estimate the elastic stiffness tensor of an isotropic rock matrix containing perfectly oriented (but randomly distributed) cracks; such a medium is transversely isotropic. The assumptions are that the cracks are small compared to the seismic wavelength, isolated, penny-shaped, and filled with weak material. This is very similar to the earlier work of Bristow (1960) and Walsh (1965a,b). Piau (1980) considered several systems of parallel cracks,and Kachanov (1980) considered a general orientation distribution.

The smoothing methods estimate the effective elastic stiffness properties for a cracked rock by combining the contributions to the elastic stiffness tensor of an isotropic rock, and of the first- and second-order dependence on crack density. The first-order method is described by

$$C_{ijkl} = C^0_{ijkl} + C^1_{ijkl} , \quad (4a)$$

and the second-order method is described by

$$C_{ijkl} = C^0_{ijkl} + C^1_{ijkl} + C^2_{ijkl} . \quad (4b)$$

In eqs. (4a) and (4b), superscripts 0, 1, and 2 denote the term sequence rather than being mathematical exponents. C_{ijkl} is the fourth-rank elastic stiffness tensor of the cracked medium,

$$C^0_{ijkl} = \lambda\delta_{ij}\delta_{kl} + \mu(\delta_{ik}\delta_{jl} + \delta_{il}\delta_{jk}) \quad (5)$$

is the stiffness tensor of the isotropic host rock, where λ and μ are the Lamé coefficients of the isotropic matrix, and δ_{ij} is the Kroneker delta ($\delta_{ij} = 1$ if i = j; otherwise $\delta_{ij} = 0$).

For cracks orientated perpendicular to the X direction (Fig. 1), Hudson (1980) derives the following to estimate C^1_{ijkl} and C^2_{ijkl}:

$$C^1_{ijkl} = -(\varepsilon/\mu)C^0_{p1ij}C^0_{q1kl}U_{pq} \quad (6)$$

is the stiffness tensor of the first-order crack term, ε is the crack density, and $U_{ij} = \text{diag}(U_{33}, U_{33}, U_{11})$, where U_{11} and U_{33} are the strain responses of a single crack, to shear and compressional stress, respectively.

In eq. 4b,

$$C^2_{ijkl} = (1/\mu)C^1_{ijmn}\chi_{mnpq}C^1_{pqkl} \quad , \quad (7)$$

contains the contribution to the stiffness tensor of the second-order crack density term, and is expressed as a function of the first-order term C^1_{ijkl}, where

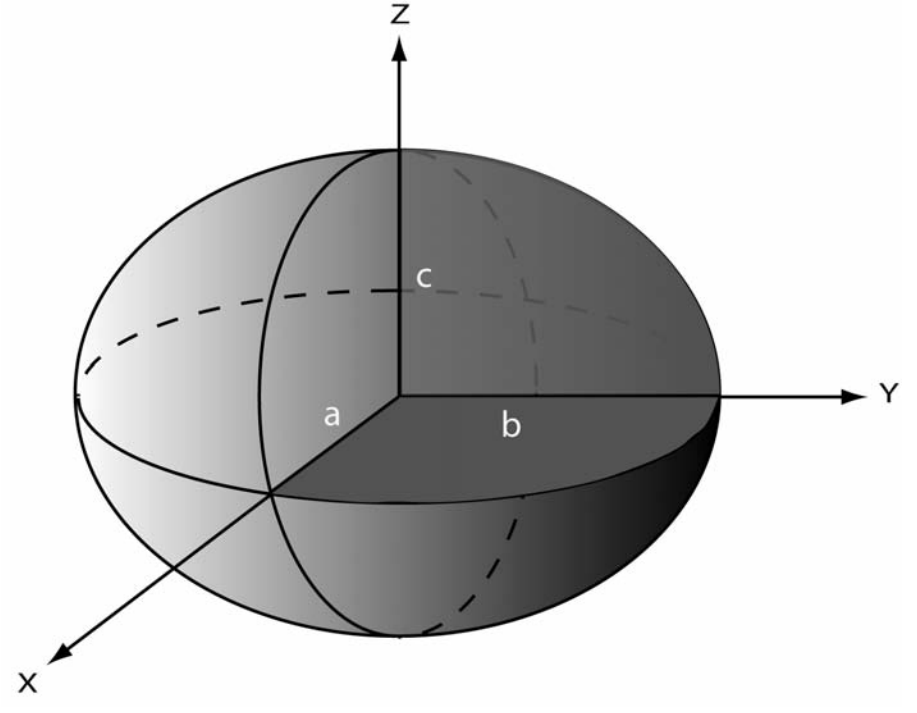

Fig. 1. Eshelby's ellipsoid model of a single inclusion.

$$\chi_{ijkl} = (1/15)[\delta_{ik}\delta_{jl}(4 + V_S^2/V_P^2) - (\delta_{ij}\delta_{kl} + \delta_{il}\delta_{jk})(1 - V_S^2/V_P^2)] \quad , \qquad (8)$$

$V_P = [(\lambda + 2\mu)/\rho]^{1/2}$ and $V_S = (\mu/\rho)^{1/2}$ are the P- and S-wave velocities, respectively, in the isotropic matrix, and ρ is bulk density of the host rock.

Hudson's first-order term C^1_{ijkl} is the contribution of individual cracks, and the second-order term C^2_{ijkl} is the contribution of crack-crack interaction, (Hudson, 1981; Crampin, 1984). Thus, the second-order approximation can be applied at higher crack density than the first-order approximation. Cheng (1993) used Padé approximations to extend Hudson's (1980, 1981) second-order model to higher crack density, to give predictions that are similar to those of the SCA and DEM methods; none of them are deterministic.

Linear slip (LS) methods

Schoenberg (1980), Kachanov (1992), Schoenberg and Sayers (1995) and Sayers and Kachanov (1995) describe a linear slip method to calculate an effective elastic stiffness tensor for fracture-induced anisotropy, using a model consisting of perfectly aligned planar fractures of infinite length and small thickness that are filled with high compliance (weak) materials.

In linear slip theory, strain is linearly related to stress, normal strain depends only on normal stress, and tangential strain depends only on tangential stress. The compliance tensor S_{ijkl} of an effective medium equals the sum of the compliance tensor S^b_{ijkl} of the matrix and the excess compliance tensor S^f_{ijkl} associated with the fractures,

$$S_{ijkl} = S^b_{ijkl} + S^f_{ijkl} \quad . \qquad (9)$$

The excess compliance tensor S^f_{ijkl} can be expressed in terms of the compliance tensor Z_{ij} of the fracture using

$$S^f_{ijkl} = \tfrac{1}{4}(Z_{ik}n_l n_j + Z_{jk}n_l n_i + Z_{il}n_k n_j + Z_{jl}n_k n_i) \quad , \qquad (10)$$

where n_i are the components of the local unit normal to the fracture surface.

If the cross section of the 3D fractures is circular, and they are aligned, then the fracture compliance can be expressed using the normal (Z_N) and tangential (Z_T) compliances (Schoenberg and Sayers, 1995) as

$$Z_{ij} = Z_T\delta_{ij} + (Z_N - Z_T)n_i n_j \quad . \qquad (11)$$

In the resulting transverse anisotropy, the compliance tensor of the fractures has three non-zero elements, two of which (Z_N and Z_T), are independent.

Many formulations have been proposed to estimate the first order crack compliance tensor assuming that the crack density is very small, so the crack interactions can be ignored. Kachanov (1980, 1992) and Sayers and Kachanov (1995) define a second-rank tensor and a fourth-rank tensor to estimate the fracture compliance Z_{ij} for circular fractures. For penny-shaped fractures, Hudson et al. (1996) present an exactly equivalent expression for the two fracture compliances: $Z_T = (\varepsilon/\mu)U_{11}$ and $Z_N = (\varepsilon/\mu)U_{33}$, where U_{11} and U_{33} are the coefficients introduced by Hudson (1981) as described in the previous section. Using different values of U_{11} and U_{33} makes the LS method applicable to a variety of fluid contents.

Hudson et al. (1996), Hudson and Liu (1999), and Liu et al. (2000) derive analytic expressions for fracture compliance for Liu's models for high crack density, for specific fracture distributions, microstructures, and geometries. Liu et al. (2000) define three fracture and crack models. Their Model 1 (Fig. 2) contains circular fractures with diameter of $2a_f$ (that is much shorter than a typical seismic wavelength). The fracture spacing is H_f, and each fracture contains a cluster of isolated smaller circular cracks with diameter $2a_c$, separated by non-circular asperities.

Liu et al. (2000) derive the excess compliance tensor for Model 1 as

$$s^f_{ijkl} = (\varepsilon/4\mu)[A'_T(\delta_{ik}n_l n_j + \delta_{jk}n_l n_j + \delta_{il}n_k n_j + \delta_{jl}n_k n_i) + 4(A'_N - A'_T)n_i n_j n_k n_l] \quad . \tag{12}$$

where

$$A'_N = A_N[1 + (3\pi/4)(\gamma_c^3/a_f)A_N\{(\lambda + \mu)/(\lambda + 2\mu)\}]^{-1} \quad , \tag{13}$$

and

$$A'_T = A_T[1 + (3\pi/16)(\gamma_c^3/a_f)A_T\{(3\lambda + 4\mu)/(\lambda + 2\mu)\}]^{-1} \quad , \tag{14}$$

where $\gamma_c = \varepsilon H_f/a_c^3$ is the number of cracks on a circular fracture plane with radius a_f,

$$A_T = U_{11}[1 + (\gamma_c a_c^2)^{3/2}U_{11}(\pi/4)(3 - 2V_S^2/V_P^2)] \quad , \tag{15}$$

and

$$A_N = U_{33}[1 + (\gamma_c a_c^2)^{3/2}U_{33}\pi(1 - V_S^2/V_P^2)] \quad . \tag{16}$$

The fracture spacing H_f (Fig. 2) is sufficiently wide that the interactions between neighboring fractures can be ignored. Crack-crack interactions occur only along the same fracture plane, as expressed by the two terms in the brackets in eqs. (15) and (16).

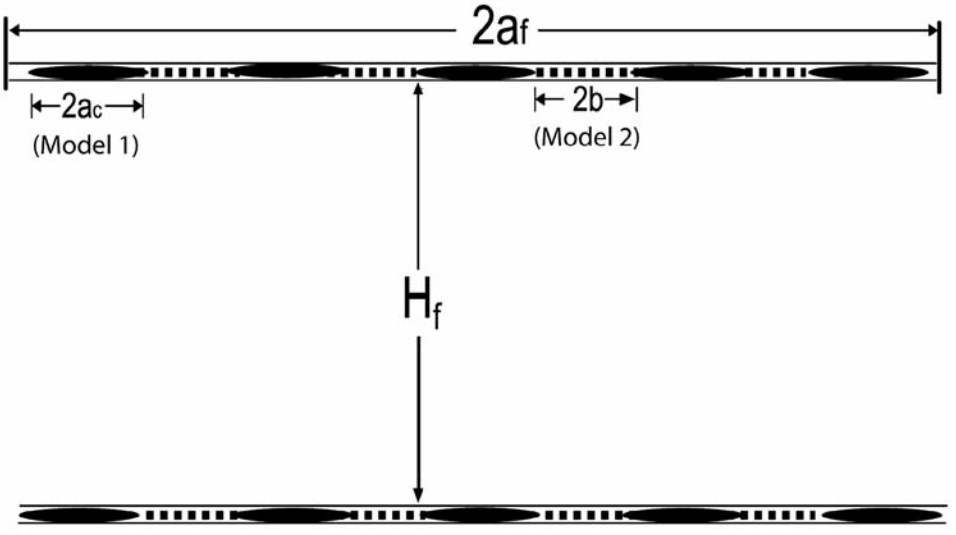

Fig. 2. Liu et al.'s (2000) fracture and crack Model 1 for the linear slip formulation. The pairs of parallel light lines are the fractures. Fractures are thin, and of circular cross section with diameter $2a_f$ and spacing H_f. Within the fractures are mixtures of cracks (the black regions) and asperities (the dotted regions). $2a_c$ is the diameter of the circular cracks, separated by (non-circular) asperities.

Liu et al. (2000) suggest that the above formulation can be reduced to Schoenberg and Sayers' (1995) (first order) LS method. If we consider only the first-order in ε, eqs. (13) and (14) become $A_N' = U_{33}$ and $A_T' = U_{11}$, which is the same as in Sayers and Kachanov (1995) and Hudson et al. (1996). Liu et al. (2000) compare this formulation with Hudson's (1980, 1981) first-order method, and suggest that they are equivalent if ε is small. Liu et al. (2000) show that if $\varepsilon \ll 1/6$ (for their specific example, for a Poisson solid), the first order LS method is equivalent to Hudson's first-order smoothing method.

T-matrix methods

This approach is an evolution of Zeller and Dederichs' (1973), Mori and Tanaka's (1973), Willis' (1977), and Castaneda and Willis' (1995) methods. Zeller and Dederichs (1973) first propose a T-matrix method of quantum scattering theory to estimate the elastic effects of individual cracks (so, this is the first-order method). Mori and Tanaka (1973) and Willis (1977) introduce the two point correlation, assuming that the crack distributions have the same shape

as the single cracks, to estimate the interactions of inclusion pairs. Castaneda and Willis (1995) extend the crack distributions to aspect ratios that are different from the crack aspect ratios. Jakobsen et al. (2003) extend the method to different shapes of crack distributions. They propose analytic solutions for specific spatial clustering patterns of the ellipsoidal inclusions (Fig. 3).The single inclusion description is the same as for Eshelby's ellipsoidal model, but the inclusion concentration may be non-dilute and their distribution is not necessarily even. This method is valid for high inclusion (crack) density, by introducing the T-matrix to describe the influence of single inclusions on the elastic stiffness tensor, and two-point correlation functions to estimate the influence of the interactions between neighboring pairs of arbitrarily-shaped inclusions. Inclusions are divided into groups with different shapes (aspect ratios). The distribution of the centers of any type of inclusion is modeled as being contained within an ellipsoid (Fig. 3). Then, two-point correlation functions having ellipsoidal symmetry are introduced to calculate the interaction between the cracks.

If the two-point correlations are same for all the crack spatial distributions the interactions between all the crack pairs are the same and the T-matrix formulation (Jakobsen et al., 2003) has the form

$$\mathbf{C}^* = \mathbf{C}^0 + (\sum_r \mathbf{t}^{(r)}\phi^{(r)})[\mathbf{I}_4 + \mathbf{G}_d(\sum_s \mathbf{t}^{(s)}\phi^{(s)})]^{-1} \quad , \tag{17}$$

where $\mathbf{C}^*$ is the effective elastic stiffness tensor, $\mathbf{C}^0$ is the stiffness tensor of the host rock, and $\mathbf{G}_d$ characterizes the interaction between an inclusion of type r at the center and other inclusions of type s surrounding it, forming an ellipsoidal region (Fig. 3). The aspect ratio of this ellipsoid (α_2) is used to describe the spatial distribution of the inclusions. $\mathbf{G}_d$ is a function of the elastic properties of the matrix, and of α_2. To compare this method with others, we use a common aspect ratio for all the inclusion interactions. $\mathbf{G}_d$ describes the same interactions for all pairs of inclusions and can be extended to different interactions between two adjacent inclusions, or among more inclusions. $\mathbf{t}^{(r)}$ (or $\mathbf{t}^{(s)}$) is the T-matrix of the r (or s) type of cracks, $\phi^{(r)} = (4\pi/3)\varepsilon^{(r)}\alpha_1^{(r)}$ is the porosity associated with type r (or s) cracks. The T-matrix

$$\mathbf{t}^{(r)} = [\mathbf{I}_4 - (\mathbf{C}^{(r)} - \mathbf{C}^0)\mathbf{G}^{(r)}]^{-1}(\mathbf{C}^{(r)} - \mathbf{C}^0) \quad , \tag{18}$$

where $\mathbf{I}_4$ is a fourth-rank identity tensor, $\mathbf{G}^{(r)}$ characterizes the effect of a single inclusion of type r having ellipsoidal symmetry, and $\mathbf{C}^{(r)}$ is the elastic stiffness tensor of inclusion type r, which is calculated from the elastic properties of the crack infill. If the aspect ratios of components r and s are different, the second term in eq. (17) needs to be calculated three times with permutations to give the r-r, s-s and r-s interactions.

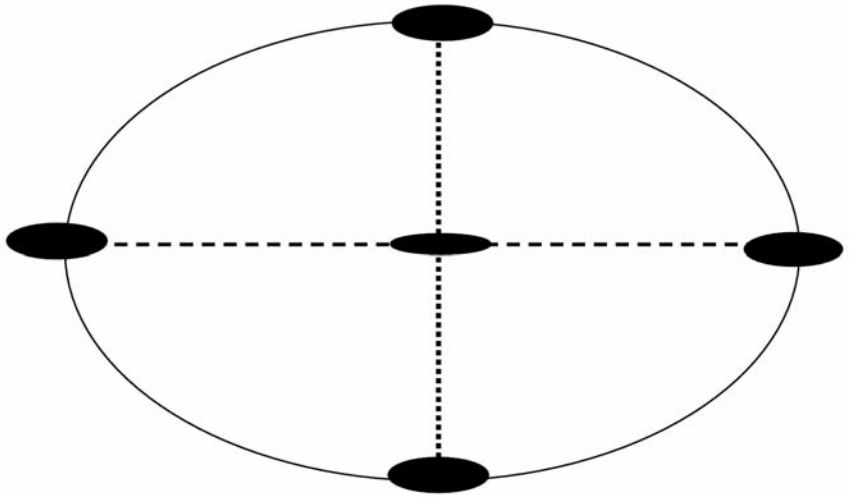

Fig. 3. Inclusion model for the T-matrix formulation. Inclusions are (the black) ellipsoids and may have different shapes (aspect ratios). The dashed lines represent the interactions between inclusions; the thickness of the dashed lines represent the strength of the interactions. The ellipse describes a regular distribution of inclusions.

Jakobsen et al. (2003) reduced eq. (17) to the second-order approximation [using the relation $(1 + \mathbf{x})^{-1} \approx (1 - \mathbf{x})$] to give

$$\mathbf{C}^* = \mathbf{C}^0 + \sum_r \mathbf{t}^{(r)}\phi^{(r)}) - [\sum_r \mathbf{t}^{(r)}]\mathbf{G}_d[\sum_s \mathbf{t}^{(s)}\phi^{(s)}] \quad , \tag{19}$$

for small inclusion density. If eq. (19) contains only the first two terms, then it is a first-order (linear) approximation. These variations are referred to below as the first- and second-order versions of the T-matrix method.

The T-matrix inclusion model contains isolated, perfectly aligned cracks with different shapes, filled with any material (and so does not have the weak material limitation of the smoothing and LS methods), and has regular crack distributions. Through the T-matrix, the anisotropic effect of a single inclusion is estimated. Through $\mathbf{G}_d$, the interaction between cracks with different shapes is estimated; the mutual interactions of more than two crack clusters can be included.

COMPARISON OF PREDICTED ELASTIC TENSORS

Although various authors have often stressed the novelty of their own methods, they have used similar principles and procedures, and hence the results

may be similar, or even equivalent, to each other under some assumptions. The fracture parametrizations, assumptions, approximations, and their consequences are important for the evaluation of the different formulations. Therefore, our comparisons focus on these aspects.

Because microstructures of real rocks cannot be accurately measured, representative values of crack density, aspect ratio, and orientation need to be defined for input to the elastic stiffness tensor calculations. Similarly, an inversion for these parameters will generally be non-unique. Different parametrizations result in different contributions of crack parameters describing the same tensor elements. Thus, it is important to know the characteristics and limitations of each theory.

An anisotropic medium may have a variety of different types of anisotropy. Although different formulations have different applicability to different types of anisotropy, for the convenience of comparison, we consider only one set of perfectly aligned, ellipsoidal, and dry cracks. Partial saturation corresponds to a three phase model and to more complicated (viscoelastic) responses, which are not considered here.

For comparison, in all the following examples, we use the same input model for the equivalent inclusion, SCA, DEM and T-matrix methods. This input model consists of perfectly aligned, dry, ellipsoidal cracks with same range of crack density (0.0 to 0.5), the same aspect ratio (0.05), and the same spatial crack distributions. Random, but statistically even, crack distributions are required by Eshelby's, SCA, DEM and Hudson's methods, so we set the aspect ratio of the spatial inclusion distributions in the T-matrix to 1.0. The parameters of the matrix that are used approximate a vertically cracked coal, as coalbed methane reservoirs (e.g., Shuck et al., 1996) are a potential application of the results of this study. The parameters used are V_P = 2500 m/s, V_S = 940 m/s, bulk density ρ = 1500 kg/m^3, and the cracks are dry. The effect, on the anisotropic elastic properties, of dry inclusions is more significant than wet ones, so using dry cracks will allow clear comparisons of the different formulations. All the effective elastic tensor elements (C^*_{ij}) in all figures are normalized [being divided by the elastic tensor elements (C^0_{ij}) of the corresponding rock matrix at $\varepsilon = 0$], so that it is convenient to see the relative differences of the moduli changes with increasing crack density.

Comparison of first-order methods: Eshelby's, Hudson's (smoothing) and Jakobsen et al.'s (T-matrix)

We use Eshelby's, Hudson's and Jakobsen's first-order methods to calculate the effective elastic stiffness tensor for a transversely isotropic medium with a horizontal symmetry axis. Eshelby (1957) considers the effect, of a single

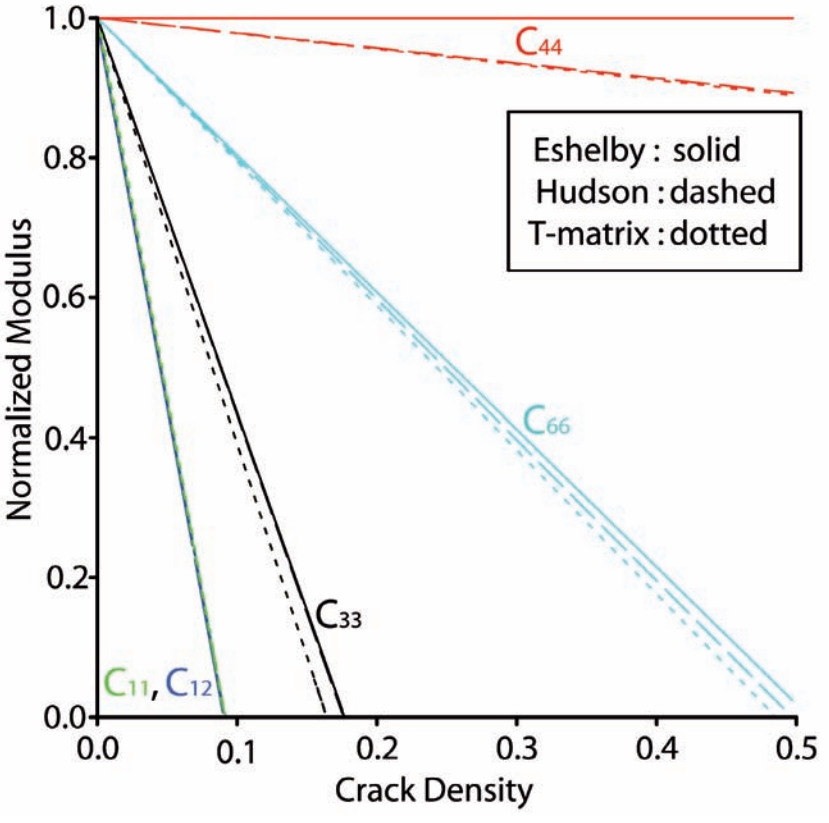

Fig. 4. Comparison of three first-order methods: the Eshelby's, Hudson's and T-matrix methods. All the triplets of curves overlap at very small crack density ($\varepsilon < 0.02$). The crack aspect ratio value used here ($\alpha_1 = 0.05$) satisfies the requirement of Hudson's method, that α_1 be small, to allow comparisons to be made with the other formulations. If α_1 is less than ~ 0.01, the curves for all three methods are overlapping and become flat (effectively isotropic). For all first order algorithms, the normalized $C_{11} \approx C_{12}$; for dry cracks, in the Hudson (1980) formulation, they are exactly equal.

inclusion, on the elastic properties of a medium. This formulation is suitable for any ellipsoidal inclusion and any infill material in the inclusion. Hudson (1980, 1981) assumes that the isolated cracks have vanishingly small aspect ratio. Hudson (1994) also extends this model to arbitrarily inclusion shapes. The individual crack effects of Hudson's (1994) method are identical to those of the T-matrix first order method.

Fig. 4 contains five triplets of curves for the normalized moduli C_{66}, C_{44}, C_{11}, C_{12}, and C_{33} for crack aspect ratio α_1 of 0.05 [which is similar to the α_1 used in the physical experiments of Rathore et al. (1991), and Ass'ad et al. (1992, 1993a, b)]. All triplets of curves are overlapped, or are very close to each other, for the whole plotted range of crack density and suggests that all the

three methods give essentially equivalent predictions. Note that, at higher ε, all the first-order methods predict unrealistically small (even negative) tensor elements. This shows the danger of using these models outside the range of assumptions for which they were derived; they should not be used at high ε.

Comparison of second-order methods: Hudson's (smoothing), and Jakobsen's (T-matrix)

Jakobsen et al. (2003) compare the second-order T-matrix approximation with Hudson's second-order smoothing approximation. They point out that the crack interaction coefficient χ_{mnpq} in eq. (7) is functionally equivalent to the product of $\mathbf{G}_d$ in equation 17 and μ. Thus, the results of these two second-order methods are effectively equivalent for small crack density ($\varepsilon < 0.03$ for our example) as shown in Fig. 5. For crack densities > 0.03, most of the second-order moduli curves (Fig. 5) have turning points, beyond which the moduli increase with increasing crack density, and so are not physical.

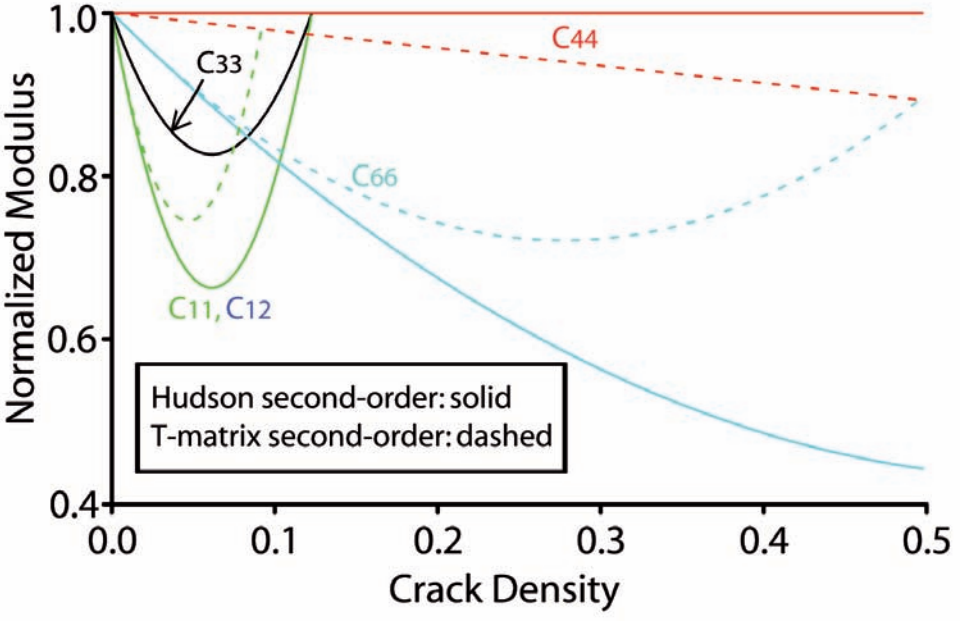

Fig. 5. Comparison of the second-order T-matrix and Hudson methods. All the pairs of curves nearly overlap at $\varepsilon < 0.03$. For all second order algorithms, the normalized $C_{11} \approx C_{12}$; for dry cracks, in the Hudson (1980) formulation, they are exactly equal.

The interactions between the inclusions enclosed within an ellipsoid and the centered inclusion (Figs. 3 and 5) are taken into account by the T-matrix. A spherically shaped crack distribution ($\alpha_2 = 1.0$, randomly but statistically evenly distributed) is implicit in Hudson's smoothing method. The T-matrix method allows superposition of different anisotropies associated with lithology and fractures. Thus, we may obtain more consistent results with the T-matrix than by using separate formulations for lithological and fracture-induced anisotropies.

The limiting crack density for validity of Hudson's second-order approximation depends on the Poisson's ratio of the rock matrix and the fluid content of the cracks. In Crampin's (1984) example for dry cracks in a matrix of the Poisson's ratio is ~ 0.29, the crack density limit is ~ 0.1. In our example, the cracks are also dry, the Poisson's ratio of the coal matrix is 0.42, which is much higher. The turning point of the second-order T-matrix curve of elastic element C_{33} is at $\varepsilon \sim 0.05$ (Fig. 5), so the crack density limit is less than 0.05 in our example. For larger Poisson's ratio, the crack densities at which the turning points occur in the second order curves (Fig. 5) are smaller.

Comparison of high-order (crack interaction) methods: SCA, DEM, T-matrix, and LS

The effective elastic stiffness curves estimated by using the T-matrix, SCA and DEM produce similar results (Fig. 6). Both SCA and DEM give plausible but slightly different results for all crack densities (Fig. 6). Plausible predictions are produced by extrapolation to high crack density, even though they are strictly valid only for random crack distributions with constant α_2 cracks. SCA and DEM quantitatively account for, but do not allow for an explicit description of, the interaction between the inclusions as they are effective medium models. The T-matrix high-order method [eq. (17)] takes physical crack-crack interactions into account.

SCA and DEM are approximate theories that seem to be qualitatively acceptable in certain cases when extrapolated to relatively high crack density. They predict decreasing moduli with increasing crack density, without being negative). Explicit inclusion of high-order interactions between cracks requires a knowledge, or higher order statistics,of the crack distribution, which are not normally available.

In creating Fig. 6, α_2 is set to 1.0, to represent a random inclusion distribution for the T-matrix high-order solution [eq. (17)]. All other parameters are the same as in the Eshelby's model calculations in Fig. 4. The T-matrix and LS methods give similar results for crack density up to ~ 0.15 for this example (Fig. 6); see Hu (2008) for more discussion.

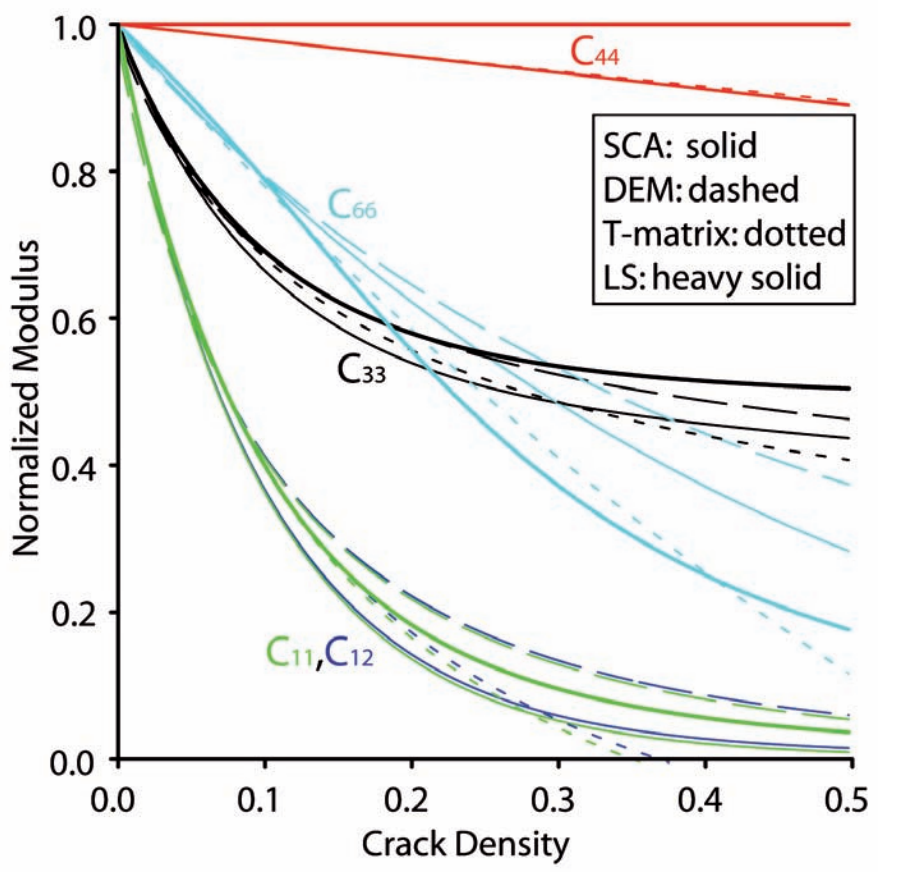

Fig. 6. Comparison of results from the T-matrix, LS, SCA and DEM methods. For the LS model, $a_c = 1.$, $a_f = 100a_c$, and $H_f = 2a_c$; for the T-matrix model, the aspect ratio of the crack distribution α_2 is 1.0.

If the crack density is sufficiently small in the LS model (Fig. 2), it approaches the configuration of the T-matrix model (Fig. 3), and the predicted elastic stiffness tensor elements are nearly the same (Fig. 6). For computing the LS curves in Fig. 6, we use Liu et al.'s Model 1, because its crack geometry is compatible with those of the T-matrix methods. The SCA, DEM and LS predictions all flatten at high crack density, and so are physically plausible, but the T-matrix solution diverges from the others and produces moduli estimates that are all generally lower than the others, especially for C_{11} and C_{12}, which become unrealistic (negative) for ε greater than ~ 0.3. This is probably a consequence of the inclusion of only nearest neighbor crack interactions in the present implementation of the high-order T-matrix solution (Fig. 3); more crack interactions correspond to less steeply decreasing moduli.

In LS, the relative lengths of the crack diameters, the asperities, the fractures, and the fracture spacings are used, while in the T-matrix methods, the aspect ratios of ellipsoidal inclusions and ellipsoidal spatial distributions of inclusions are used. At low crack density, the moduli are not sensitive to the geometrical details of the various models. At higher crack density, the spatial distribution of the cracks becomes important. Of all the moduli, C_{66} shows the greatest relative variation between models at high crack density. The C_{44} prediction by LS in Fig. 6 is flat because it is not dependent on crack porosity in this model.

DISCUSSION

The crack models in each of the theoretical formulations considered above are different, but with some key similarities. The main common feature is that the cracks are perfectly aligned. The crack models of Eshelby's, SCA, DEM and high-order T-matrix formulations all have ellipsoidal shapes with any aspect ratio, the infilling materials may be gas (or dry), liquid or solid. The inclusion distributions of Eshelby's, SCA and DEM formulations are random but statistically even, but may have special patterns in the T-matrix formulation. The models in Hudson's smoothing and LS formulations both have flat, circular cracks filled with weak materials, but the cracks are randomly but statistically evenly distributed for Hudson's formulation, while in LS, the cracks are distributed in specific patterns as described by Liu et al. (2000).

For dilute cracks, the cracks are isolated, and crack-crack interaction is ignored. When the cracks are dilute, the elastic stiffness tensor values decrease linearly with increasing crack density, as in Eshelby's (1957) single equivalent inclusion method, Hudson's, and the first-order T-matrix approximations (Fig. 4). Crack-crack interactions must be considered when the cracks are non-dilute. Hudson's second-order approximation, SCA, DEM, T-matrix and LS methods can all approximate non-dilute behavior, but give different predictions with increasing crack density.

If the crack density is larger than ~ 0.1 (Crampin, 1994), crack characterization becomes more complex because crack-crack interactions become important. The fractures are also likely to be highly irregular in shape (aspect ratio) and orientation. Therefore, complex and significant crack-crack interactions will be generated. If cracks coalesce, the effective dimensions increase and may become longer than the seismic wavelength and so violate the assumption of the medium being elastic.

Even the most general T-matrix and LS methods may be inaccurate at high crack densities as no model with a simple geometrical crack description can accurately represent the complexity of real fracture systems. For Liu's

high-order LS method, fracture spacings are assumed to be large enough that the interactions between the fractures can be ignored. This assumption is possible only for limited crack density. For high crack density, average fracture spacings become small thus the interactions between the fractures cannot be ignored (Davis and Knopoff, 1995; Dahm and Becker, 1998; Liu, 2007). Comparison with experimental data is needed to define which theoretical predictions work best in practice. Quantitative descriptions of the microstructures of cracked rocks, as seen in the laboratory, need to be explicitly included for the accuracy of the models to be evaluated. We could not find any published examples of physical experiments to determine tensor elements for crack density $\varepsilon > 0.1$; no such evaluation is apparently yet done. Peacock et al. (1994) do have crack density measurements $\varepsilon > 0.1$, but these are for randomly oriented (not aligned) cracks.

The crack shape (the crack aspect ratio α_1) is another important property of the microstructure since it determines the porosity and permeability associated with the fractures. It is also critical to anisotropic effects. If $\alpha_1 = 1.0$, the inclusions are spherical, the medium is isotropic, and there are only two rather than five independent elastic moduli (as $C_{33} = C_{11}$, $C_{66} = C_{55} = C_{44}$ and $C_{12} = C_{13} = C_{23} = C_{11} - 2C_{44}$). These moduli all decrease with increasing crack density or crack porosity. If α_1 is vanishingly small, again there is no significant anisotropic effect produced, and all five normalized elastic moduli curves are essentially flat (set $\phi_{n,p} = 0$ in eq. (2), or $\phi^{(r,s)} = 0$ in eq. (17). Any shape of ellipsoidal inclusions with aspect ratios ranging from zero to infinity may be included in the Eshelby, SCA, DEM, and T-matrix methods, but only circular cracks are considered in the LS and Hudson's smoothing methods and only for aspect ratios that are vanishingly small.

Crack distributions have significant influence on the anisotropic effects of the elasticities when crack density is large. When crack density is large, the average distances between cracks are small. Thus, the crack interactions become strong and need to be included. SCA, DEM and Hudson's smoothing methods are applicable for randomly distributed cracks. In Liu et al.'s (2000) LS methods, all the cracks are confined to large fracture planes and the fracture spacings are sufficiently wide that the crack interactions along the fracture strike dominate over other directions. In the T-matrix method, the spatial distributions of cracks are ellipsoids (Fig. 2); if they are spherical, the cracks are randomly distributed. In this paper we discuss only perfectly aligned cracks. However, the cracks in a real rock may be not perfectly aligned; for example, there may be two sets of cracks (which are not rare in real rocks) (Hudson, 1986), or the orientation of the cracks may have a normal distribution around a dominant direction (Hornby et al., 1994; Jakobsen et al., 2003).

The infill material in the cracks also influences the anisotropy. Hudson's (1980, 1981) and LS methods are applicable only to weak infill materials. Other

methods do not have such constraints, and so have the potential for application to non-crack induced anisotropy, such as anisotropy in shale. Models for partially water-saturated cracks are developed by Hudson (1988) and Jakobsen (2004).

Permeability anisotropy is dependent on cracks, but it cannot be directly studied in the present context, because all of these formulations are defined only for unconnected cracks and fractures, and thus have zero permeability. In real rock, there is a contribution to the anisotropy of permeability only from connected cracks. A small number of large cracks (still small compared to a seismic wavelength) and a large number of small cracks can have the same crack density, and hence, produce the same elastic stiffness anisotropy, but different permeability.

Not all of the theoretical formulations have the same parametrization and this limits their applicability. For example, in Liu et al.'s (2000) high-order LS method, the cracks are penny-shaped, so it can not be applied to study a carbonate reservoir with high aspect ratio vugs. For the convenience of comparison, all the models used above contain perfectly aligned cracks. However, some of the formulations can be applied to more complex cases which are common in nature; for example, Hudson's smoothing formulation can be applied to two sets of cracks if we ignore the interactions between them, and the T-matrix formulation can be applied to imperfectly aligned cracks (Hornby et al., 1994; Sayers, 1994).

Computational simulations with finite difference or finite elements for specific realizations of cracked media (Grechka and Kachanov, 2006a, b; Kachanov, 1992; Mauge and Kachanov, 1994; Saenger and Shapiro, 2002; Saenger et al., 2004) are perhaps the most reasonable way to produce a basis for evaluating the accuracy of the theoretical solutions. Numerical solutions can predict both static and dynamic moduli, which can be very different (e.g., Saenger et al., 2006). Numerical simulations also address the issue of irregularly shaped cracks; the usual crack density parameters assume only circular shapes. Irregular crack geometries and their effect on the effective compliance are discussed by Kachanov (1994), Grechka and Kachanov (2006d) and Sevostianov and Kachanov (2002).

These results set the stage for production of synthetic seismograms for various crack configurations via input, of the corresponding elastic stiffness tensors, to numerical solutions of the anisotropic elastic wave equation (e.g., Ramos-Martínez and McMechan, 2000). If the elastic stiffness tensors for two models are similar, they will produce similar seismograms, regardless of the details of the properties of the crack sets and their distributions. This also opens the possibility for estimation of crack properties, and their uncertainty, by anisotropic full wavefield inversion.

CONCLUSIONS

The two main types of elastic effects of cracks in a rock are individual crack effects and crack interactions. At small crack density, the average distances between the cracks are large, the crack-crack interactions can be ignored, but, at high crack density, they are strong and can become complicated.

All the theoretical formulations above produce very similar predictions of moduli at small crack densities ($\varepsilon < 0.03$), but differ significantly from each other at high crack densities. This indicates that all these methods predict the same individual crack effects, which are also consistent with the physical and numerical experiments. So, the predictions of the individual crack effects are accurate, but the predictions of the crack interaction effects are qualitatively reasonable only by the formulations that contain crack interactions. Interactions may be included either implicitly, as in the SCA and DEM methods, or explicitly, as in the LS and T-matrix methods. Each crack model only partly resolves the problems, because each uses different assumptions about the microstructure geometry and crack interactions. There is a clear need for extensive lab measurements to be performed to test the theoretical models; much remains to be done.

A variety of crack parameters such as shapes, spatial distributions, orientation distributions, and fluid contents, all play important roles in the effective elastic properties, and all are visible in the corresponding synthetic seismograms (Hu, 2008).

ACKNOWLEDGMENTS

The research leading to this paper was supported by the Sponsors of the UT-Dallas Geophysical Consortium, and a teaching assistantship from the Department of Geosciences at the University of Texas at Dallas. This paper is Contribution No. 1197 from the Department of Geosciences at the University of Texas at Dallas.

REFERENCES

Ass'ad, J.M., Tatham, R.H. and McDonald, J.A., 1992. A physical model study of microcrack-induced anisotropy. Geophysics, 57: 1562-1570.

Ass'ad, J.M., Riveros, C., Sismos, S.A., Kamel, M.H. and McDonald, J.A., 1993a. Ultrasonic velocity measurements in a cracked solid: experimental versus theory. Expanded Abstr., 63rd Ann. Internat. SEG Mtg., Washington D.C.: 762-764.

Ass'ad, J.M., Tatham, R.H. and McDonald, J.A., 1993b. A physical model study of scattering of waves by aligned craks: comparison between experiment and theory. Geophys. Prosp., 41: 323-339.

Benveniste, Y., 1986. On the Mori-Tanaka method for cracked solids. Mechan. Res. Communic., 13: 193-201.

Bristow, J.R., 1960. Microcracks and the static and dynamic elastic constantsof annealed heavily cold-worked metals. Brit. J. Appl. Phys., 11: 81-85.

Budiansky, B. and O'Connell, R.J., 1976. Elastic moduli of a cracked solid. Internat. J. Solids Struct., 12: 81-97.

Castaneda, P.P. and Willis, J.R., 1995. The effect of spatial distribution on the effective behavior of composite materials and cracked media. J. Mechanics Phys. Solids, 43: 1919-1951.

Cheng, C.H., 1978. Seismic Velocities in Porous Rocks: Direct and Inverse Problems. Sc.D. Thesis, Massachusetts Institute of Technology, Cambridge.

Cheng, C.H., 1993. Crack models for a transversely isotropic medium. J. Geophys. Res., 98: 675-684.

Crampin, S., 1984. Effective anisotropic elastic constants for wave propagation through cracked solids. Geophys. J. Roy. Astronom. Soc., 76: 135-145.

Crampin, S., 1994. Comments on "Crack models for a transversely isotropic medium" by C.H. Cheng and comment by C.M. Sayers. J. Geophys. Res., 99: 11749-11751.

Crampin, S., McGonigle, R. and Bamford, D., 1980. Estimating crack parameters from observations of P-wave velocity anisotropy. Geophysics, 45: 345-360.

Dahm, T. and Becker, Th., 1998. On the elastic and viscous properties of media containing strongly interacting cracks. Pure Appl. Geophys., 151: 1-16.

David, C., Menendez, B. and Darot, M., 1999. Influence of stress-induced and thermal cracking on physical properties and microstructure of La Peyratte granite. Internat. J. Rock Mechan. Mining Sci., 36: 433-448.

Davis, P.M. and Knopoff, L., 1995. The elastic modulus of media containing strongly interacting antiplane cracks. J. Geophys. Res., 100: B9, 18253-18258.

Douma, J., 1988. The effect of the aspect ratio on cracked-induced anisotropy. Geophys. Prosp., 36: 614-632.

Eshelby, J.D., 1957. The determination of the elastic field of an ellipsoidal inclusion, and related problems. Proc. Roy. Soc. London, Series A, Mathematical and Physical Sciences, 241: 376-396.

Grechka, V. and Kachanov, M., 2006a. Seismic characterization of multiple fracture sets: Does orthotropy suffice? Geophysics, 71: D93-D105.

Grechka, V. and Kachanov, M., 2006b. Effective elasticity of rocks with closely spaced and intersecting cracks. Geophysics, 71: D85-D91.

Grechka, V. and M. Kachanov, 2006c. The influence of crack shapes on the effective elasticity of fractured rocks. Geophysics, 71: D153-D160.

Grechka, V. and Kachanov, M., 2006d. The influence of crack shapes on the effective elasticity of fractured rocks: A snapshot of the work in progress, Tutorial. Geophysics, 71: W45-W58.

Gupta, I.N., 1973. Seismic velocities in rock subjected to axial loading up to shear fracture. J. Geophys. Res., 78: 6936-6942.

Hadley, K., 1975. V_P/V_S anomalies in dilatant rock samples. Pure Appl. Geophys., 113: 1-23.

Hashin, Z., 1988. The differential scheme and its application to cracked materials. J. Mechan. Phys. Solids, 36: 719-734.

Hoening, A., 1979. Elastic moduli of a non-randomly cracked body. Internat. J. Solids Struct., 15: 137-154.

Hornby, B.E., Schwartz, L.M. and Hudson, J.A., 1994. Anisotropic effective-medium modeling of the elastic properties of shales. Geophysics, 59: 1570-1583.

Hu, Y., 2008. Stiffness tensor models for high crack density with application to seismic modeling and imaging of coal and carbonate reservoirs. Ph.D. Dissertation, The University of Texas at Dallas.

Hu, Y. and McMechan, G.A., 2009. Comparison of effective stiffness and compliance for characterizing cracked rocks. Geophysics, 74: D49-D55.

Hudson, J.A., 1980. Overall properties of a cracked solid. Mathemat. Proc. Cambridge Philosoph. Soc., 88: 371-384.

Hudson, J.A., 1981. Wave speeds and attenuation of elastic waves in material containing cracks. Geophys. J. Roy. Astronom. Soc., 64: 133-150.

Hudson, J.A., 1986. A higher order approximation to the wave propagation constants for a cracked solid. Geophys. J. Roy. Astronom. Soc., 87: 265-274.

Hudson, J.A., 1988. Seismic wave propagation through material containing partially saturated cracks. Geophys. J., 92: 33-37.

Hudson, J.A., 1994. Overall properties of a material with inclusions or cavities. Geophys. J. Internat., 117: 555-561.

Hudson, J.A., Liu, E. and Crampin, S., 1996. The mechanical properties of materials with interconnected cracks and pores. Geophys. J. Internat., 124: 105-112.

Hudson, J.A. and Liu, E., 1999. Effective elastic properties of heavily faulted structures. Geophysics, 64: 479-485.

Jakobsen, M., 2004. The interacting inclusion model of wave-induced fluid flow. Geophys. J. Internat., 158: 1168-1176.

Jakobsen, M., Hudson, J.A. and Johansen, T.A., 2003. T-Matrix approach to shale acoustics. Geophys. J. Internat., 154: 533-558.

Jakobsen, M. and Johansen, T.A., 2000. Anisotropic approximations for mudrocks: A seismic laboratory study. Geophysics, 65: 1711-1725.

Kachanov, M., 1980. Continuum model of medium with cracks. J. Engineer. Mechan. Div., ASCE, 106(EM5): 1039-1051.

Kachanov, M., 1992. Effective elastic properties of cracked solids: Critical review of some basic concepts. Appl. Mechanics Rev., 45: 305-336.

Kachanov, M., 1994. Elastic solids with many cracks and related problems. In: Hutchinson J. and Wu, T. (Eds.), Advances in Applied Mechanics. Academic Press, New York: 256-426.

Lin, S.C. and Mura, T., 1973. Elastic fields of inclusions in anisotropic media (II): Physica Status Solidi (a), 15: 281-285.

Liu, E., 2007. Introduction, Special issue on seismic anisotropy, Part I - Fracture Characterization. J. Seismic Explor., 16: 105-114.

Liu, E., Hudson, J.A. and Pointer, T., 2000. Equivalent medium representation of fractured rock. J. Geophys. Res., 105: 2981-3000.

Lo, T.W., Coyner, K.B. and Toksöz, M.N., 1986. Experimental determination of elastic anisotropy of Berea sandstone, Chicopee shale, and Chelmsford granite. Geophysics, 51: 164-171.

Mauge, C. and Kachinov, M., 1994. Effective elastic properties of on anisotropic material with arbitrarily oriented interacting cracks. J. Mechan. Phys. Solids, 42: 561-584.

Mori, T. and Tanaka, K., 1973. Average stress in matrix and average elastic energy of materials with misfitting inclusions. Acta Metallurg., 21: 571-574.

Nishizawa, O., 1982. Seismic velocity anisotropy in a medium containing oriented cracks - transversely isotropic case. J. Phys. Earth, 30: 331-347.

Nur, A. and Simmons, G., 1969. Stress-induced velocity anisotropy in rock: an experimental study. J. Geophys. Res., 74: 6667-6674.

O'Connell, R.J. and Budiansky, B., 1974. Seismic velocities in dry and saturated cracked solids. J. Geophys. Res., 79: 5412-5426.

O'Connell, R.J. and Budiansky, B., 1977. Viscoelastic properties of fluid saturated cracked solids. J. Geophys. Res., 82: 5719-5735.

Peacock, S., McCann, C., Sothcott, J. and Astin, T.R., 1994. Seismic velocities in fractured rocks: an experimental verification of Hudson's theory. Geophys. Prosp., 42: 27-80.

Piau, M., 1980. Crack-induced anisotropy and scattering in stressed rocks. Internat. J. Engineer. Sci., 19: 549-568.

Ramos-Martínez, J., Ortega, A.A and McMechan, G.A., 2000. 3-D seismic modeling for fractured media: Shear-wave splitting at vertical incidence in one and multiple layers. Geophysics, 65: 211-221.

Rathore, J.S., Fjaer, E., Holt, R.M. and Renlie, L., 1991. Experimental versus theoretical acoustic anisotropy in controlled cracked synthetics. Expanded Abstr., 61st Ann. Internat. SEG Mtg., Houston: 687-690.

Rathore, J.S., Fjaer, E., Holt, R.M. and Renlie, L., 1994, P- and S-wave anisotropy with controlled crack geometry. Geophys. Prosp., 43: 711-728.

Saenger, E.H., 2007. Comment on "Comparison of the non-interaction and differential schemes in predicting the effective elastic properties of fractures media" by V. Grechka. Internat. J. Fracture, 146: 291-292.

Saenger, E.H., Krüger, O.S. and Shapiro, S.A., 2004. Effective elastic properties of randomly fractured soils: 3D numerical experiments. Geophys. Prosp., 52: 183-195.

Saenger, E.H., Krüger, O.S. and Shapiro, S.A., 2006. Effective elastic properties of fractured rocks: Dynamic vs. static considerations. Expanded Abstr., 76th Ann. Internat. SEG Mtg., New Orleans: 1948-1951.

Saenger, E.H. and Shapiro, S.A., 2002. Effective elastic velocities in fractured media: A numerical study using the rotated staggered finite-difference grid. Geophys. Prosp., 50: 183-194.

Salganik, R.L., 1973. Mechanics of bodies with a large number of cracks. Mechan. Solids, 8(4): 135-143.

Sayers, C.M., 1994. Reply of "Comment on 'Crack models for a transversely isotropic medium' by C.H. Cheng and comment by C. M. Sayers". J. Geophys. Res., 99(B6): 11753-11754.

Sayers, C.M. and Kachanov, M., 1995. A simple technique for finding effective elastic constants of cracked solids for arbitrary crack orientation statistics. Internat. J. Solids and Struct., 27: 671-680.

Schoenberg, M., 1980. Elastic wave behavior across linear slip interfaces. J. Acoust. Soc. Am., 68: 1516-1521.

Schoenberg, M. and Douma, J., 1988. Elastic wave propagation in media with parallel fractures and aligned cracks. Geophys. Prosp., 36: 571-590.

Schoenberg, M. and Sayers, C.M., 1995. Seismic anisotropy of fractured rock. Geophysics, 60: 204-211.

Sevostianov, I. and Kachanov, M., 2001. Elastic compliance of an annular crack. Internat. J. Fract., 110: L31-L34.

Sevostianov, I. and Kachanov, M., 2002. On the elastic compliances of irregularly shaped cracks. Internat. J. Fract., 114: 245-257.

Sheng, P., 1990. Effective-medium theory of sedimentary rocks. Phys. Review B, 41: 4507-4511.

Shuck, E.L., Davis, T.L. and Benson, R.D., 1996. Multicomponent 3-D characterization of a coalbed methane reservoir. Geophysics, 61: 315-330.

Thomsen, L., 1986. Weak elastic anisotropy. Geophysics, 51: 1954-1966.

Thomsen, L., 1995. Elastic anisotropy due to aligned cracks in porous rocks. Geophys. Prosp., 43: 805-829.

Vavakin, A.S. and Salganik, R.L., 1975. Effective characteristics of nonhomogeneous media with isolated inhomogeneities. Mechan. Solids, 10: 58-66 (English translation from Izvestia AN USSR, Mekhanika Tverdogo Tela, 10: 65-77.

Walsh, J.B., 1965a. The effect of cracks on the compressibility of rocks. J. Geophys. Res., 70: 381-389.

Walsh, J.B., 1965b. The effect of cracks on uniaxial compression of rocks. J. Geophys. Res., 70: 399-411.

Wang, Z., 2002. Seismic anisotropy in sedimentary rocks, part 2: Laboratory data. Geophysics, 67: 1423-1440.

Willis, J.R., 1977. Bounds and self consistent estimates for the overall properties of anisotropic composites. J. Mechan. Phys. Solids, 25: 185-202.

Zeller, R. and Dederichs, P.H., 1973. Elastic constants of polycrystals, Physical Status solid (b), 55: 831-843.